J. Membrane Biol. 41, 197–224 (1978)

Do Light-Induced Changes in the Membrane Potential of *Nitella* Reflect the Feed-Back Regulation of a Cytoplasmic Parameter?

Ulf-Peter Hansen

Institut für Angewandte Physik, Neue Universität, Haus N61A, 23 Kiel, W.-Germany

Received 6 July 1977; revised 10 October 1977; revised again 24 January 1978

Summary. Kinetic studies of the linearized response of membrane potential in *Nitella* to light have revealed the existence of a feedback loop in the pathway of light action. Its existence can hardly be seen in the time course of the responses to dark/light transitions. However, making use of sine waves as input signals and employing a computeraided evaluation has resulted in finding complex time constants in the transfer function of the light effect which point out the existence of a feedback loop. Besides, sometimes spontaneous oscillations with periods of about 1 hr have been observed. It is shown that this system is different from that one reported in literature to be related to cytoplasmic streaming. By measuring the electrical low-frequency impedance, it has been demonstrated that it is not the purpose of the system to control membrane potential, even though secondary effects of the injected current have been found. It seems to be reasonable to assume that this system is involved in the control of a biochemically relevant parameter like the cytoplasmic pH by means of adjusting the balance of counteracting transmembrane transport processes.

In green plants light acts via photosynthesis on the ion transport and thus on the electrical properties at the plasma membrane. Starting from the papers of MacRobbie (e.g., 1966) it has been believed for several years that photosynthesis exerts its control over the ion fluxes at the plasma membrane by supplying the energy that fuels the ion pumps (*see* Raven, 1969). However, now there are many observations indicating that the concept of energy supply *per se* is not sufficient to account for all experimental findings (*see* Raven, 1974).

Thus feedback regulations have been postulated for the concentrations of NO_3^- and Cl^- (Cram, 1973) and of Na^+ (Robinson, 1968). In the case of the cytoplasmic pH, indications of a feedback regulation are expected to show up in the kinetic behavior of the membrane potential, because biochemical "pH-stats" like that one proposed by Davies (1973) are not efficient in balancing all the pH-shifts caused by metabolic

0022-2631/78/0041-0197 $05.60
© Springer-Verlag New York Inc. 1978

activities, and thus the transmembrane transport of protons or hydroxyl ions is believed to be a major means of maintaining cytoplasmic pH (Raven & Smith, 1974; 1976). Proton fluxes are supposed to be electrogenic in green plants (Spanswick, 1972; 1974, Felle & Bentrup, 1976) as well as in fungi (Slayman, Long & Lu, 1973). Pallaghy and Lüttge (1970) and Andrianov *et al.* (1971) have demonstrated that the light-induced changes in membrane potential are related to proton fluxes.

The assumption of a feedback control of the cytoplasmic pH is reasonable. On the one hand, there is the need for such a control mechanism, because the pH is the most important parameter determining the activity of enzymes and because a pH shift may be caused by several metabolic processes like photosynthetic CO_2-fixation, nitrogen assimilation, excess organic acid synthesis used in turgor regulation (*see* Raven & Smith, 1974; 1976), or proton extrusion from photosynthesizing chloroplasts (Heldt *et al.*, 1973).

On the other hand, there are experimental findings which point out the regulation of the cytoplasmic pH like the coupling between the spatially separated HCO_3^-- and OH^--transport sites (Lucas, 1976) or the constancy of the pH in the cytoplasm, when changes in the pH of the bathing medium shift the pH in the more distant vacuole (*see*, e.g., Walker & Smith, 1975).

The hypothesis that the pH in the cytoplasm is controlled by means of the electrogenic transmembrane transport of protons or hydroxyl ions is supported by the observation of Davis (1974) that the light-induced changes in cytoplasmic pH and in membrane potential in *Phaeoceros laevis* are of like characteristics. In this paper it will be shown that a refined analysis of the light-induced responses of the potential reveals an oscillatory component which points out the existence of a feedback loop.

Materials and Methods

General

If not otherwise stated, *Nitella mucronata A.Br. Miquel* was used in the experiments. The cells had been collected from a pond in the botanical garden of Kiel and were kept in plastic basins in the lab in Forsberg (1965) medium *II* for about three years at a temperature of 17 °C and at a light intensity of 1 W/m^2 (16 hr per day). For the experiments in Fig. 4 and in Fig. 5 *Nitella translucens* was used (a gift of Dr. Vredenberg, Wageningen).

Details of the experimental set-up and of the procedure of measuring frequency responses have been described in previous papers (Hansen, Warncke & Keunecke, 1973;

Hansen, 1974). Briefly, single internodal cells of *Nitella* were placed in a small Lucite vessel perfused by artificial pond water containing 0.1 mM/liter KCl, 1.0 mM/liter NaCl, and 0.1 mmole/l $CaCl_2$. Before entering the vessel the solution flowed through a coil embedded in water of adequate temperature, which was 17 °C, if not otherwise stated. The changes in membrane potential were evoked by the red light of the luminescence diode MV4H of Monsanto ($\lambda = 680$ nm, bandwidth = 40 nm) by modulating the light intensity by sine waves of frequencies ranging from 16 cycles/min to 1 cycle/4 hr. The modulation depth was 50%; that means that the light intensity varied between 0.5 and 1.5 W/m^2 during the course of a sine wave. This modulation depth and this range of intensity had been proved to yield linearized responses by means of experiments which will be published in a separate paper. The low frequencies were generated by a digital sine wave generator (Hansen, 1970), which also served as a master clock for the data acquisition.

Recording Apparatus

The membrane potential of the *Nitella* cell was measured by conventional microelectrodes filled with 1 *n* KCl connected to high-impedance FET amplifiers. After adequate amplification, the light-induced changes in membrane potential were recorded on a four-channel chart recorder (*see* Hansen *et al.*, 1973) and besides, after analog to digital conversion (1 bit = 100 μV), punched on a paper tape (6 to 36 samples per period of a sine-wave cycle depending on the signal to noise ratio). The tapes were fed into the X-8 computer of the Kieler Rechenzentrum, and the Fourier coefficients of the light-induced changes were calculated. The fundamental waves were used for the frequency responses (*see* Fig. 2), and the higher harmonics served as a proof for linearity. Before Fourier analysis, the drift in the membrane potential was eliminated by subtracting a polynomial of the third degree obtained by regression analysis. The calculation of the kinetic data of the transfer functions [*see* Eq. (4)] was carried out by means of the ALGOL program of Strobel (1968), modified for the dialog with the PDP-10 computer. Some more details of this approach are given by Hansen (1974), and a more detailed description dealing with the problems of linearity and drift elimination will be presented in a separate paper.

Methods of the Analysis of Time-Courses

The physical background of the analysis of time courses. The temporal behavior of biochemical and biological reactions is determined by the differential equations originating from the law of mass action. This is demonstrated by the Eqs. (A2a) to (A2c), (A21) and (A22) in the Appendix. Diffusion in compartmental systems or filling of reservoirs are described by the like differential equations and are included in this kind of analysis (Berman, Weiss & Shahn, 1962). However, normally biological systems are nonlinear [*see* Eq. (A20)] leading to a set of nonlinear differential equations like Eqs. (A21) and (A22). From such a set of equations the response of the system to a stimulus can be calculated. However, in this paper we have to deal with the "inverse problem" (Lee, 1968). We want to investigate an unknown mechanism by the observation of its temporal behavior. This approach will be successful only if the system is simplified considerably, e.g., by the method of linearization.

Linearization. As it is illustrated by the Eqs. (A23) to (A26) in the Appendix, linearization can be achieved by the following experimental procedure: The system is kept under steady-state conditions, and the perturbations applied have to be so small

that the terms of higher order may be neglected (pseudo first-order system; *see* Eigen & De Mayer, 1963; Eigen, 1968; Milsum, 1966).

In the case of the measurements presented here, linearity was checked by watching whether the amplitude of the output signal was in straight-line proportion to the amplitude of the input signal, and whether the phase-shift of a sinusoidal signal was independent of the amplitude. The characteristic data gained from a linearized response are the time constants.

Curve fitting in the "time domain". Very often the time constants (τ_i) are gained from responses to a step-wise change of the environmental conditions by fitting the linear response $f_{(t)}$ by a superposition of exponentials

$$f_{(t)} = w_0 + w_1 \exp\left(-\frac{t}{\tau_1}\right) + w_2 \exp\left(-\frac{t}{\tau_2}\right) + \cdots \tag{1}$$

Curve fitting in the "frequency domain". The accuracy of determining the time constants can be improved by using sine waves as an input signal (e.g., *see* the "fast-pole problem" Milsum, 1966, p. 213). In chemical systems the benefits of the sine waves are normally not utilized because the addition of an agent is much easier to perform than the sinusoidal modulation of a concentration. However, in the case of the light effect in *Nitella*, the light intensity can be modulated easily by sine waves of frequencies ranging from 16 cycles/min to 1 cycle/4 hr. At about 13 to 19 frequencies, differing by an octave or by half an octave, the ratios of the input to output amplitudes $A_{(f)}$ (A in Fig. 2) and the phase shifts $\varphi_{(f)}$ were recorded. In order to apply the curve-fitting routine of Strobel (1968), $A_{(f)}$ and $\varphi_{(f)}$ were combined to create the "complex transfer function" $H_{(jf)}$.

$$H_{(jf)} = A_{(f)} \exp(j\varphi_{(f)}). \tag{2}$$

As it is demonstrated by the examples in the Appendix [*see* Eqs. (A5) to (A9)], $H_{(jf)}$ is the quotient of two polynomials of the frequency f (or p). By calculating the roots of the polynomials, $H_{(jf)}$ may be rearranged to the form of Eq. (3).

$$H_{(jf)} = H_0 \frac{(1-pn_1)(1-pn_2)\ldots}{(1-p\tau_1)(1-p\tau_2)\ldots} \tag{3}$$

with H_0 being the "dc amplification", $p = 2\pi j f$, $j = \sqrt{-1}$, f the frequency. The constants n_k in the numerator are called to "inverse zeros", the constants τ_i in the denominator are identical to the time constants τ_1 in Eq. 1 [*see* Milsum, 1966; Capellos & Bielski, 1972 ("operational method")]. The mathematical transition from Eq. (1) to Eq. (3) and vice versa is mediated by the Laplace transform (Milsum, 1966).

The meaning of the time constants. The time constants are the roots of the denominator of $H_{(jf)}$, and thus they are a more or less complicated function of the elementary reaction rates [*see* Eqs. (A5) to (A9)] and of the concentrations of the reactants in the case of nonlinear systems [*see* Eqs. (A20) to (A24)]. Also diffusion processes or fillings of reservoirs may contribute to the actual value of a measured time constant.

Thus the determination of the time constants is just a first step in the analysis of a system, which may already provide knowledge of that kind presented in Fig. 8. The next step has to be based on the method of "extended kinetics". That is studying the influence of different treatments on the values of the time constants.

Complex time constants. Sometimes, pairs of the time constants turn out to be complex numbers consisting of each a real component and an imaginary component. The two members of a pair have the same real component and differ by the sign of the imaginary component (*see* τ_2 and τ_3 in Table 1). In the Appendix it is shown that complex time constants point out the existence of feedback loops. Inserting complex time constants into Eq. (1) results in a damping factor and an oscillation [*see* Eq. (5)]. Their relation to this more familiar phenomenon will be discussed below.

Spontaneous oscillations. In that case the real component of the complex time constants is about zero; thus there is no damping. This is the most convincing evidence for the existence of feedback loops. In the case of *Nitella* it has been employed by Nishizaki (1968) and Lefebvre and Gillet (1970). The oscillations reported by Ogata and Kishimoto (1976), however, demonstrate that this conclusion needs some comments, as discussed below.

Damped oscillations. If the real component is not zero, but smaller than the imaginary component, damped oscillations will be caused by environmental stimuli, as, e.g., the application of drugs (Metlicka & Rybova, 1967; Gradmann & Slayman, 1975), irradiation with X-rays (Hansen, 1967), or temperature (Spanswick, 1972). By means of that method most of the feedback systems in metabolism were detected (e.g., *see* Higgins, 1967).

Hidden oscillations. With increasing magnitude of the real component of the complex time constants, the oscillations fade out and can no longer be identified. In that case the responses of the system have to be subjected to a powerful mathematical analysis in order to check for complex time constants. Due to the better resolution provided by the treatment in the "frequency domain" mentioned above, frequency responses like that one shown in Fig. 2 will be analyzed by a computer aided curve-fitting procedure.

Results

1. *The Existence of a Feedback Loop in the Pathway of Light Action as Revealed by the Kinetic Analysis of the Light-Induced Changes in Membrane Potential*

The problem. Figure 1 displays the response of membrane potential in *Nitella* to a step-wise change in light intensity. It can hardly be stated whether the bump at 32 min is indicating a damped oscillation. Thus the approach outlined in the section "hidden oscillations" has to be applied.

Experiments. Single internodal cells of *Nitella* were illuminated by light whose intensity was modulated by sine waves of different frequencies. This kind of illumination induced sinusoidal changes in membrane potential. The amplitudes and the phase shifts of these responses were plotted *vs.* the frequency of the modulation in plots like that one displayed in Fig. 2. The experimental procedure differed from that one normally employed by the application of sine waves and by the small

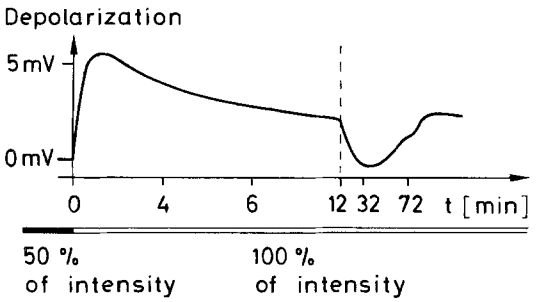

Fig. 1. Response of the membrane potential in *Nitella mucronata* to an increase in light intensity from 1 W/m^2 to 2 W/m^2 (white light, 17 °C). Without a refined analysis, the oscillatory component can hardly be identified

modulation depth instead of light/dark transitions. These conditions allow the application of the mathematical analysis described below.

Mathematical treatment of the experiments. In the sections above and in the Appendix it has been shown that Eq. (3) is the only adequate kind of functions for the mathematical approximation of frequency responses like that one exhibited in Fig. 2. The curve-fitting procedure can be performed by means of the ALGOL program of Strobel (1968) which results in the following transfer function:

$$H_{(jf)}=\frac{H_0(1-pn_1)(1-pn_2)(1-pn_3)}{(1-p\tau_1)(1-p\tau_2)(1-p\tau_3)(1-p\tau_4)(1-p\tau_5)(1-p\tau_6)}. \qquad (4)$$

The smooth lines in Fig. 2*A* are gained by this procedure. Table 1 displays the mean values of the n_i and τ_i evaluated from about 40 experiments at three different temperatures.

Interpretation of the results of the curve-fitting procedure. In this paper we are not interested in discussing the curve-fitting routine. We are only interested in that part of Eq. (4) which points out the existence of a feedback loop: that are the conjugate complex time constants τ_2 and τ_3 (*see* Table 1). In the Appendix it is shown that straightforward reactions are not capable of creating complex time constants. The occurence of the complex time constants in Eq. (4) and Table 1 indicates that there is a back flow from a subsequent step to a preceding one in the chain of reactions mediating the light effect on membrane potential. This back flow is called feedback.

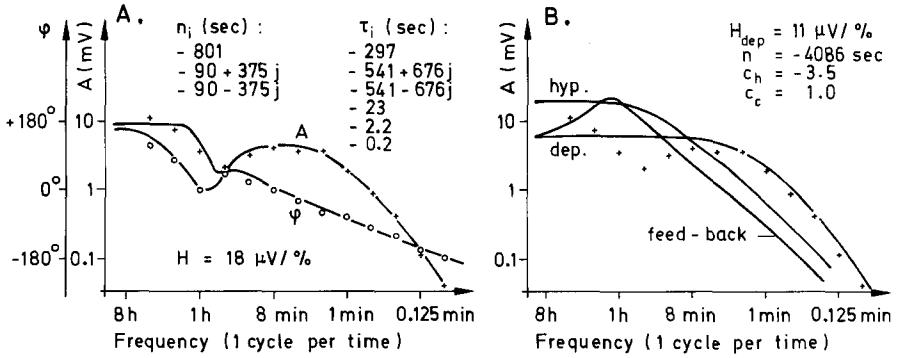

Fig. 2. (*A*): Curve fitting applied to the frequency responses of the action of light on the membrane potential in *Nitella mucronata*. The experimental data are presented by crosses (A = amplitude) and circles (φ = phase). (*B*): Splitting the frequency response of the amplitude A into the three components due to Eq. (9) and to the model in Fig. 8. The crosses represent the same data as in *A*, indicating that at the high-frequency slope the depolarizing pathway alone fits the experimental data, whereas at lower frequencies all three pathways determine the light-induced changes

Table 1. Averaged values of the kinetic data of Eq. (4) gained from experiments performed at different temperatures[a]

	n_1	n_2/n_3	τ_1	τ_2 and τ_3	τ_4	τ_5	τ_6	H_0	No. of exp.	τ_d (min)	$1/f_0$
7 °C	640	95 ± 811 j	−611	−257 ± 1165 j	−40	−3.7		33	8	184	128
17 °C	1213	73 ± 443 j	−344	−239 ± 640 j	−23	−3.1	−0.2	34	18	64	76
27 °C	773	35 ± 277 j	−315	−53 ± 372 j	−12	2.5		42	8	89	40
σ_M	3	3.5 1.5	4	2.1 1.6	1.5	1.6	2.5	4			

[a] The signs of n_1 and of the real components of n_2 and of n_3 were sometimes negative (n_1: 10 to 20%, $n_{2/3}$: 25 to 50%). The variance σ_M is given as a factor. The unit of H_0 is μV/% modulation. The experiments performed at 7 and 27 °C did not comprise enough measurements at high frequencies, thus τ_6 was not determined in those cases.

Implications of the data in Table 1 for the appearance of oscillations. Eq. (4) may be transformed into the time-domain, resulting in an equation of the kind of Eq. (1). Of special interest is that term of Eq. (1) which is related to the complex time constants τ_2 and τ_3, because it describes a damped oscillation. It is called $f_{23(t)}$.

$$f_{23(t)} = V_0 \exp(t/\tau_d) \sin(2\pi f_0 t + \varphi) \tag{5}$$

with t being the time. V_0 is the scaling factor and φ is the phase shift, determined by the zeros of Eq. (4). The values of both quantities have to

be calculated by means of the Laplace transform of Eq. (4), but they are of no interest in this discussion. τ_d is the damping factor and f_0 is the frequency of the oscillation. Their relations to τ_2 or τ_3 are given by Eqs. (6) and (7) (Re = real component of, Im = imaginary component of):

$$2\pi f_0 = \mathrm{Im}\, 1/\tau_2 = -\mathrm{Im}\, 1/\tau_3 \tag{6}$$

$$\tau_d = 2/\mathrm{Re}\, 1/\tau_2 = 2/\mathrm{Re}\, 1/\tau_3. \tag{7}$$

Inserting the time constants of Table 1 into Eqs. (5) to (7) (*see* Table 1, the last two columns) shows that the damping factor τ_d causes a decay to $1/e$ of the initial amplitude within one period. Thus under normal conditions pronounced oscillations are not observed in the time course of the light responses of membrane potential in *Nitella* (*see* Fig. 1), and a computer analysis like that one presented here has to be applied in order to detect the oscillatory component.

Additional experimental support for the existence of the feedback loop. In the above section it is demonstrated that under normal conditions there are no pronounced oscillations. However, the real components of τ_2 (τ_3) exhibit scatter, which is much larger in single cells than indicated by the factor of 2.1 given by the mean value of σ_M in Table 1. If the real components become very small or even zero, long lasting or even spontaneous oscillations will occur. These oscillations, which may be taken as a welcome confirmation of the kinetic analysis, have been observed, indeed. Though the experimental conditions which favor these oscillations are still unknown in detail, it seems that they occur pre-

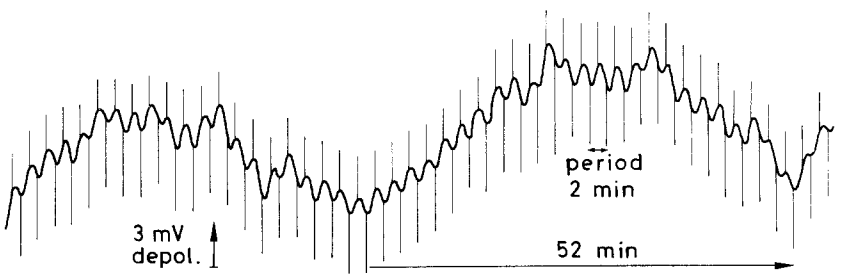

Fig. 3. Spontaneous oscillation of the membrane potential with a period of 52 min, which corresponds to the value of 66 min, which is calculated from the mean value of τ_2 in Table 1 by means of Eq. 6. The superimposed sine wave with a period of 2 min is caused by the modulation of the light intensity due to the measurement of a frequency response. The markers indicate maximum and minimum light intensity in order to indicate the phase shift. The resting potential is about 90 mV. The oscillation occurred before the cell died

ferably in cells being under stress. Fig. 3 displays such a spontaneous oscillation which arose in a dying cell during the measurement of the light-induced changes in membrane potential caused by a sine wave of a period of 2 min/cycle.

2. *Comparison with Other Oscillatory Phenomena*

An argument against the above interpretation. Ogata and Kishimoto (1976) have published some experiments which point out the existence of an oscillation of the membrane potential which is strongly correlated to cytoplasmic streaming. (It will be called "streaming oscillation" in the following text). Though the authors do not know exactly what is the origin of this oscillation, they believe that the results favor the explanation that it is caused by an agent circulating with the streaming cytoplasm and acting on membrane potential (*personal communication*). In this case the oscillation may not be taken as an evidence for the existence of a feedback control system as it has been done in the case of the oscillatory phenomenon described in the preceding section.

Experimental findings excluding that τ_2 and τ_3 are related to the streaming oscillation. Spontaneous oscillations with periods in the range of seconds and in the range of 5 to 30 min have occurred randomly during the measurements of the frequency responses of the light effect in *Nitella*. Two examples are shown in Fig. 4. Whereas by virtue of the time-scale, the quick oscillations can *a priori* be excluded from being identical to the oscillatory phenomenon related to τ_2 and τ_3, additional experiments are required in the case of the slow oscillations. In earlier experiments, when these slow oscillations were observed, it was checked several times, whether there is any dent in the frequency responses (*see* Fig. 2) of the light effect in the range of the frequency of the spontaneous oscillation. The result was negative, and f_0 [*see* Eq. (6)] was always found to be lower than the frequency of the spontaneous oscillation by at least a factor of two. Unfortunately, the length of the cells and the velocity of the cyclosis were not recorded.

Thus after getting knowledge of the publication of Ogata and Kishimoto (1976), the experiments were repeated in a two-compartment chamber like that one used by the two authors. Because the two halves of the cells were placed in different "ponds", which were electrically insulated by an air gap, differences in the membrane potentials of the two halves could be recorded by external electrodes emerged into the two ponds. They will be called "longitudinal potentials".

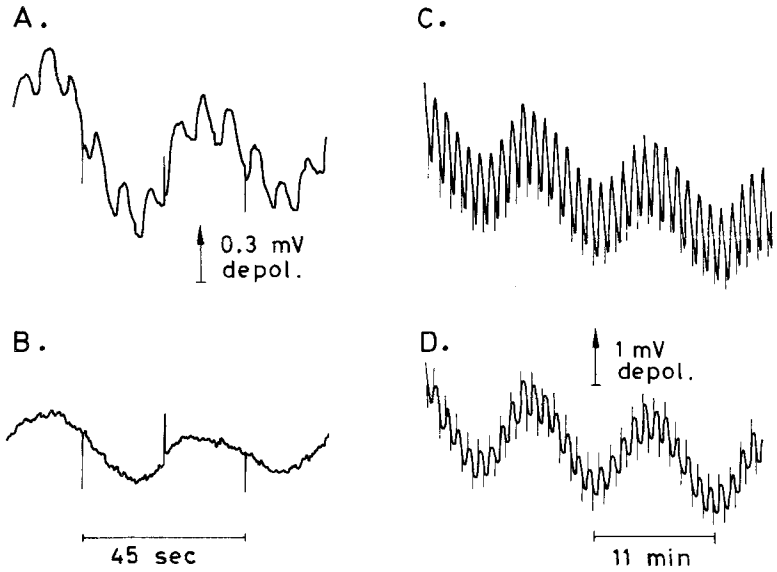

Fig. 4. Spontaneous oscillations of the membrane potential of *Nitella translucens*, which occurred during the measurement of the frequency responses of the light effect. The oscillations are superimposed by the light-induced signal. The markers indicate maximum and minimum light intensity. (*A*): Oscillation with a period of 7 sec. Transmembrane potential measured by a microelectrode. The period of the light-induced signal is 45 sec. (*B*): The transmembrane 7-sec oscillation is not seen in the longitudinal potential measured by external electrodes. (*C*): Oscillation with a period of 11 min, transmembrane potential. The period of the light-induced signal is 1 min. (*D*): The 11-min oscillation is a longitudinal oscillation

The "transmembrane potential" was measured by means of a microelectrode inserted into one half of the cell. The light for the induction of the light-evoked changes in membrane potential was focused onto that half of the cell where the microelectrode was inserted. The unequal illumination caused a longitudinal light-induced signal which was welcome as a test for the electrical insulation of the two ponds.

By means of the comparison between the transmembrane potential (Fig. 4*A*) and the longitudinal potential (Fig. 4*B*), it is seen that the quick oscillation is a transmembrane effect, whereas the slow oscillation is a longitudinal oscillation (Fig. 4*D*), as it is the streaming oscillation found by Ogata and Kishimoto (1976). Also the period was always close to the value T_{OK} calculated from the formula given by the two authors:

$$T_{OK} = 2\,l/v \tag{8}$$

with l being the length of the cell and v the velocity of the cyclosis. In the case of Fig. 4*D*, the measured period T_m was 11 min, the length of the cell

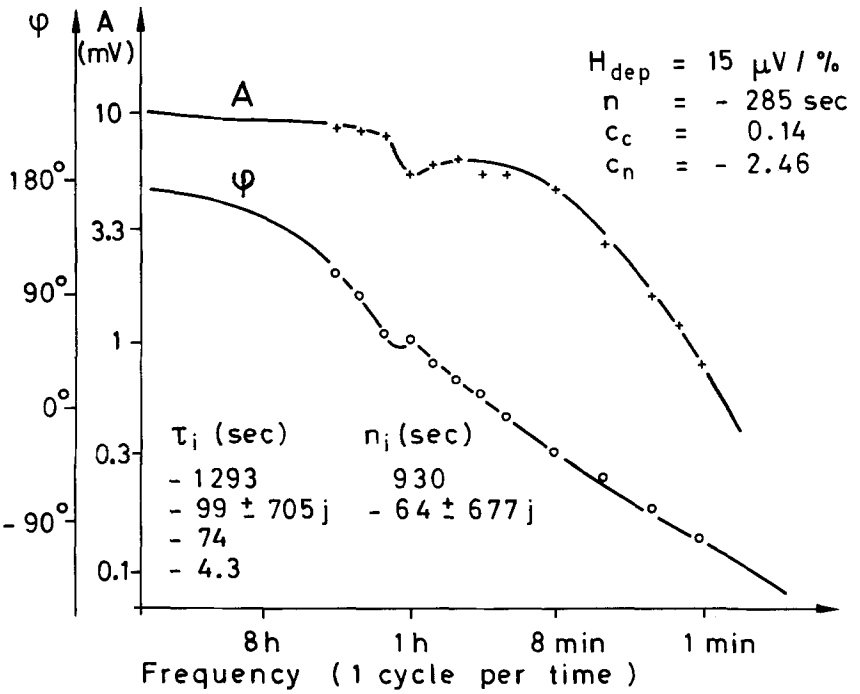

Fig. 5. Frequency responses of the light effect of the amplitude (A) and of the phase (φ) measured in the cell that displayed the oscillation shown in Fig. 4 *C* and *D*. No dents are seen in the range of frequencies of about 1 cycle/11 min. The resonance frequency [*see* Eq. (6)] is 1 cycle/70 min. The kinetic data corresponding to those in Tables 1 and 2 are displayed in the figure. Red light, intensity = 1 W/m^2, $T = 17$ °C

2.5 cm, and $v = 60$ μm/s, resulting in $T_{OK} = 14$ min. The period increases in longer cells, e.g., in a cell with $l = 5.5$ cm, T_m was 30 min, and T_{OK} was 27 min.

In those cells where the streaming oscillation was observed, the frequency responses of the light-induced changes were measured and evaluated by the method described in the preceding section. It was found that f_0 [*see* Eq. (6)] was always lower than $1/T_m$ by at least a factor of two. Fig. 5 displays the frequency response of that cell which exhibited the oscillations shown in Fig. 4 *D*. f_0 being 1 cycle/70 min is quite different from $1/T_m$ being 1 cycle/11 min. Again it is seen that the frequency response in Fig. 5 does not exhibit any irregularity at 1 cycle/11 min.

The magnitudes of the time constants in Fig. 5 demand an additional remark, because they are significantly slower than those of Table 1 (e.g., τ_4 in Fig. 5 is 74 sec instead of 23 sec in Table 1). This was

found in all cells of *Nitella translucens*, when the experiments were done shortly after their arrival from Dr. Vredenberg in Wageningen. After having been in Kiel for a month, they became faster.

3. *Is the Membrane Potential Controlled by the Feedback Loop?*

Considerations initiating the above question. Most of the workers in the field of plant electrophysiology are interested in what is the biological meaning of the membrane potential. This question is still open, though a first approach to that question may be provided by the finding of cotransport systems which are driven by membrane potential in *Neurospora* (Slayman & Slayman, 1974; Slayman, Slayman & Hansen, 1977; Hansen & Slayman, 1978) and *Chlorella* (Komor & Tanner, 1977). Thus everytime, when the action of a feedback system shows up in membrane potential, the question arises whether this feedback system has to control membrane potential. (If nature installs a feedback loop to control membrane potential, this should be a hint that membrane potential is of some interest for the cell).

If the feedback system is involved in the regulation of membrane potential, it is expected to compensate changes in membrane potential caused by the injection of an electrical current within the time scale given by τ_2 and τ_3. Some observations reported by other authors indicate that there may be an effect of this kind. Walker and Hope (1969) found that the current needed to clamp membrane potential became less after some minutes. In *Nitella* long time constants occurred, when the plasma membrane was hyperpolarized (Kishimoto, 1966; Bradley & Williams, 1967). Gradmann (1975) attributed a "late capacity" of about $3000\,\mu F/cm^2$ to an interaction between the ATP-pool and the membrane potential, whereas Noyes and Rehm (1971) suggested an accumulation of ions in reservoirs in the frog skin as an explanation for the long time constants they found.

Experiments excluding the involvement of the observed feedback loop in the regulation of the membrane potential. The considerations outlined above stimulated the following experiments. An additional microelectrode was inserted into the *Nitella* cell, and a current was injected causing a displacement of the membrane potential of some mV. In Fig. 6 the response of the membrane potential to switching on the current is shown. Figure 7 displays the frequency response of membrane potential to sinusoidal currents, and is nothing else but a measurement of the electrical membrane impedance performed in a very low frequency range.

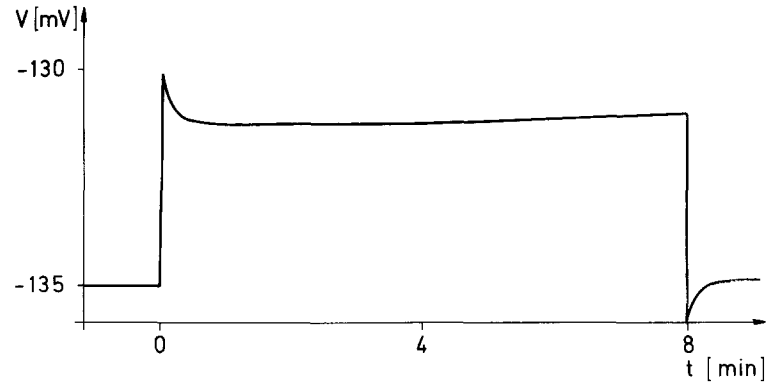

Fig. 6. The response of the membrane potential in *Nitella mucronata* to a long current pulse of 0.5 μA/cm². Red light, intensity = 1 W/m², $T = 17$ °C

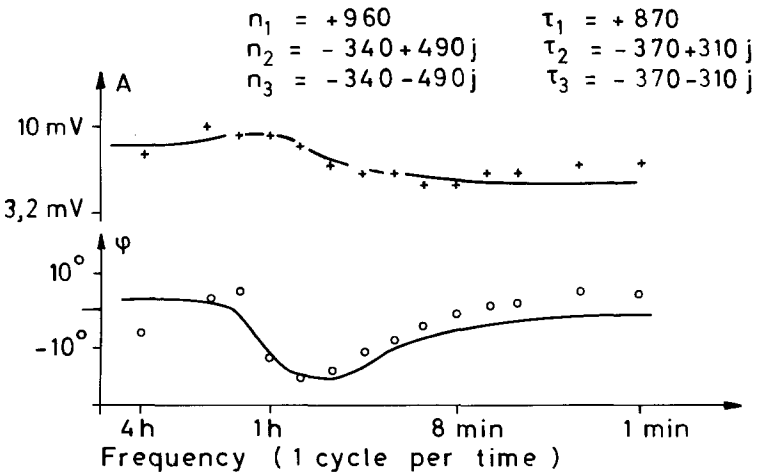

Fig. 7. The frequency responses of the amplitude (A) and of the phase (φ) of the changes in the membrane potential of *Nitella mucronata* caused by the injection of sinusoidal currents with an amplitude of 0.5 μA/cm² and with frequencies ranging from 1 cycle/min to 1 cycle/4 hr. The experimental data are fitted by the same routine as the data of Figs. 2 and 5. The kinetic data are displayed in the figure. Red light, intensity = 1 W/m², $T = 17$ °C

The experiments of both kinds demonstrate very clearly that the feedback system is not designed in order to control membrane potential. In Fig. 6, the deviation of the membrane potential is far from being canceled within 8 min. Figure 7 exhibits only minor dents in the frequency responses of phase and amplitude in the range of 1 cycle/hr,

which corresponds to 10 min in the time scale. However, the small dents in Fig. 6 and in Fig. 7 indicate that there are secondary effects of the injected current. Subjecting five frequency responses of the electrical impedance (*see* Fig. 7) to the same curve fitting routine as in the case of Fig. 2*A* resulted in complex time constants being of the same magnitude as τ_2 and τ_3. The mean value is $480 \pm 520j$ (sec) and within the range given by the variance of τ_2 and τ_3 in Table 1. These findings will be discussed in more detail below.

Discussion

Existence of a Feed-Back Loop

In the introduction it has been outlined that it is reasonable to assume that the pH of the cytoplasm is controlled by means of the transmembrane transport of protons or hydroxyl ions. Since this kind of transport is believed to be electrogenic, the action of the control system is expected to become obvious in the kinetic behavior of the membrane potential. This suggestion is strongly supported by the observation of Davis (1974) that the light-induced changes of the pH in the cytoplasm and of the membrane potential are of like characteristics.

The contribution of the experiments described in this article is to provide evidence that a kinetic analysis of the light-induced changes in membrane potential indeed reveals the existence of a feedback loop. Thus it is proved that these changes in membrane potential reflect the action of a control system. This statement could be achieved by performing the experiments under such conditions that the results could be subjected to a mathematical treatment.

However, demonstrating the existence of the feedback loop is no proof that this feedback system is really the hypothetical one proposed to control the pH in the cytoplasm. Additional information has to be gained. Regarding this, it may be interesting that Flemström (1973) has found oscillations of similar frequency (45 min) in the potential and in the hydrogen fluxes of *frog* gastric mucosa.

Creating a model from Rearranging Eq. (4) *and from the Comparison of Light-Induced Changes in Potential and in Resistance*

At first, the kinetic analysis may be extended a little bit further by dealing with the so-called "inverse problem". That is searching for

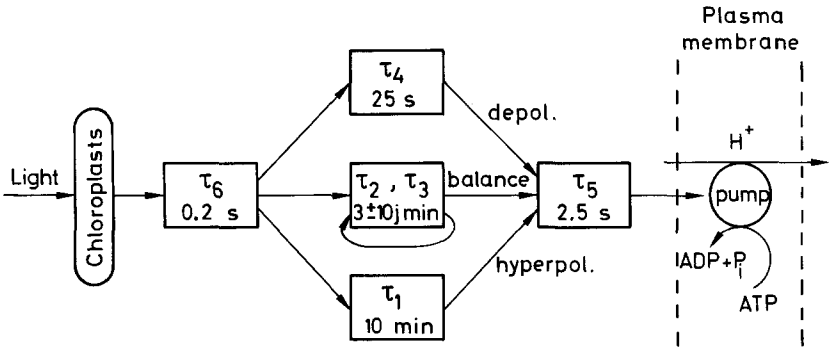

Fig. 8. The parallel-pathway model of the action of light on membrane potential due to Eq. (9)

arrangements of reactions labeled by the time constants of Table 1, which are capable of creating the measured frequency response. The inverse problem is ambigious. Different arrangements of the reactions can result in the same frequency response. The correct model has to be selected by providing more information by additional experiments.

In our case, the model shown in Fig. 8 displays the essential features of other possible models. In order to account for the experimental findings presented by Eq. (4), τ_5 and τ_6 have to be in series with the slow reactions, because there are no zeros at high frequencies. The locations of τ_6 and of τ_5 before and behind the branching point, however, are completely arbitrary. The slow reactions have to be in parallel in order to generate the zeros n_1 to n_3. Especially, this arrangement can easily create the observed scatter of the signs of these zeros (*see* Table 1) by small changes in c_c and c_h in Eq. (9). Equation (9) is mathematically identical to Eq. (4), but rearranged in such a manner that the structure of the model in Fig. 8 becomes obvious.

$$H_{(jf)}=\frac{H_{\mathrm{dep}}}{(1-p\tau_6)}\left\{\frac{1}{(1-p\tau_4)}+\frac{c_c(1-pn)}{(1-p\tau_2)(1-p\tau_3)}+\frac{c_h}{(1-p\tau_1)}\right\}\frac{1}{(1-p\tau_5)}. \quad (9)$$

The sum in the bracket of Eq. (9) implies that the measured frequency responses in *Nitella* (*see* Fig. 2*A*) result from the superposition of the frequency responses of three parallel pathways. There are a slow pathway ($\tau_1=10$ min) hyperpolarizing with light (*see* the negative sign of c_h in Table 2), a quick depolarizing pathway ($\tau_4=25$ sec), and a feedback loop labeled by τ_2 and τ_3. c_c and c_h are measures of the relative contributions of the feedback loop and of the hyperpolarizing pathway, respectively, to

Table 2. The splitting parameters of Eq. (9) calculated from the experiments displayed in Table 1[a]

	n[sec]	σ_M	No.	C_c	σ_M	No.	C_h	σ_M	H_{dep} [μV/%]	σ_M
7 °C	−2798	5.5	6	−0.09	3.8	3	−2.61	1.8	25.3	1.9
	+2053	1.6	2	+0.48	8.8	5				
17 °C	−2110	3.2	9	−0.67	1.8	5	−2.2	2.2	44.9	1.7
	+ 525	3.8	8	+0.42	4.8	12				
27 °C	+ 993	4.9	6	−0.14	2.7	4	−2.4	2.9	63.5	1.5
				+0.26	1.5	2				

[a] Splitting was done before averaging. In the case of n and c_c data with the same sign were averaged. The scatter in sign is believed to originate from the special function of the feedback loop as a final adjustment

the whole effect, compared with the contribution H_{dep} of the depolarizing pathway. The averaged values of c_c, c_h, H_{dep} and the hypothetical zero n are given in Table 2. Figure 2*B* demonstrates the splitting of the whole frequency response of Fig. 2*A* into its three components. After the splitting procedure, the characteristic phenomenon of the feedback loop becomes obvious, the resonance peak.

The model in Fig. 8 may be elaborated a little bit further by additional information gained from the simultaneous measurement of the light-induced changes in membrane potential and in resistance (*see* Hansen & Keunecke, 1977). The changes in resistance are found to be too small in comparison with the changes in potential as to be related to changes in the passive permeabilities. In detail, the comparison of these two quantites demonstrates that the depolarizing pathway is due to slowing down an electrogenic pump with light, and the hyperpolarizing one is due to speeding up this or another pump. Starting from the generally accepted assumption that proton extrusion is the predominant electrogenic active transport in Nitella (Spanswick, 1972; 1974), the following hypothesis may be furnished.

Switching on the light causes changes in the metabolism which result in an increase of the pH of the cytoplasm, as it has been observed by Davis (1974). The quick pathway slows down proton extrusion in order to balance the change of the pH. After the induction period the metabolism releases proton (see Davis, 1974) which have to be extruded by stimulating the pump via the hyperpolarizing pathway. Both pathways achieve a crude control of the pH. The fine adjustment has to be performed by the

feedback loop. Since it is a feedback loop, it is highly sensitive to the actual state of the cell. Evidence for this special function of the feedback loop is supplied by the enormous scatter in c_c (*see* Table 2), because a mechanism performing a fine adjustment has to support sometimes the hyperpolarizing pathway and sometimes the depolarizing one.

The next two features discussed here provide no positive evidence for the model of Fig. 8, but they are necessary, because they exclude possible objections.

Relation to Cyclosis

The results of the experiments illustrated by Figs. 4 and 5 prove that the streaming oscillation and the oscillatory phenomenen due to τ_2 and τ_3 are related to different mechanisms. However, it will not be surprising, if a relation of the feedback loop and of the cyclosis will be found, because Lucas and Dainty (1977) are supporting the idea that cytoplasmic streaming is involved in the transport of hydroxylions to the transport sites and thus in the regulation of the pH.

With regard to that aspect it may be worthwhile to point out that in Fig. 4*C* a small influence of the streaming oscillation on the amplitude of the light-induced signal is found. However, it is not believed that the HCO_3^-/OH^- system is identical to the pump in Fig. 8, because that system is not activated at the low light intensities of about $1\ W/m^2$ (Lucas, 1975*a*–*b*). This holds for our cells, too, because the increased complexity of the kinetics of the changes in membrane potential evoked by higher light intensities points out the activation of additional processes (Hansen *et al.*, 1973; Hansen & Keunecke, 1974).

Relation to Membrane Potential

The results of Figs. 6 and 7 demonstrate that the feedback loop is not interested in controlling the membrane potential. This is similar to the findings of Gradmann and Slayman (1975) who have demonstrated that the feedback loop which shows up in the membrane potential of *Neurospora* is not involved in the regulation of membrane potential.

Changing the Cytoplasmic pH by Injecting a Current

Due to the measurements of Kitasato (1968), the membrane current in *Nitella* is mainly carried by protons. Thus the injection of a current by means of a microelectrode filled with KCl will result in an exchange of

K^+ for H^+ in the cytoplasm. One hypothesis explaining the occurrence of the complex time constants in Fig. 7 is the assumption that the injected current changes the cytoplasmic pH and thus stimulates the feedback loop. The following calculation will give an estimate whether this change in pH may be of sufficient magnitude. It is a very crude estimation, because some data are uncertain or have to be taken from measurements in other tissues.

Assuming a thickness of the cytoplasmic layer of 5 μm, a current of $0.5\,\mu A/cm^2 = 5\,pmole/cm^2\,sec$ of H^+ results in a change of the H^+-concentration of 10 mmol/liter within 1000 sec. If the buffer capacity of the cytoplasm in *Nitella* is similar to that in *Neurospora* (Slayman & Slayman, 1968), 12 mmol/liter of H^+ cause a pH shift of 0.3 at pH 6.4. In *Phaeoceros laevis* a pH shift of 0.3 is related to a change in membrane potential of about 15 mV (Davis, 1974). This change is of sufficient magnitude to explain the dents in Fig. 7, even if the major part of the protons is lost by the exchange with the bathing medium or with the vacuole.

These investigations have been granted by the Deutsche Forschungsgemeinschaft. The author is indebted to Prof. Dr. C.L. Slayman and Dr. J. Warncke, New Haven, Dr. habil D. Gradmann, Tübingen, Dr. P. Keunecke and Prof. Dr. K. Vanselow, Kiel, for helpful discussions, and to Dr. W.J. Vredenberg, Wageningen, for supplying *Nitella translucens*.

Appendix

1. Proof that Straightforward Reactions, Including Simple Backward Reactions, do not Create Complex Times Constants

Since the existence of complex time constants like τ_2 and τ_3 in Table 1 is used as an indicator for the existence of a feedback loop, it seems to be worthwhile to present a proof that chains of straightforward reactions like that one shown in Eq. (A1) are not capable of creating complex time constants.

$$A_{n+1} \rightleftharpoons A_n \rightleftharpoons A_{n-1} \rightleftharpoons \cdots \rightleftharpoons A_4 \rightleftharpoons A_3 \rightleftharpoons A_2 \rightleftharpoons A_1 \xrightarrow{k_e} \quad \text{(A1)}$$

In Eq. (A1) all reactions are first-order reactions or pseudo first-order reactions. By virtue of the linearization the scheme above also holds for more complicated reactions, because enzymatic concentrations, etc., are comprised in the reaction constants $k_{l,m}$ which describe the rate of

conversion from A_l to A_m (*see* Eigen & De Mayer, 1963). It should be pointed out that in Eq. (A1) the order of the indices is unusual, since No. 1 is the last reactant; however, this order is favorable for the following proof based on induction.

At first we calculate the transfer functions (frequency responses) of the short chain A_4 to A_1. The law of mass action leads to the following set of differential equations in the time domain:

$$\frac{da_3}{dt}=k_{43}a_4-(k_{34}+k_{32})a_3+k_{23}a_2 \tag{A2a}$$

$$\frac{da_2}{dt}=k_{32}a_3-(k_{23}+k_{21})a_2+k_{12}a_1 \tag{A2b}$$

$$\frac{da_1}{dt}=k_{21}a_2-(k_{12}+k_e)a_1. \tag{A2c}$$

The differential Eqs. (A2a)–(A2c) are located in the time domain, because the a_i are functions of the time, and have the meaning of concentrations. We are interested in frequency responses which are located in the frequency domain, where the A_i are functions of the generalized frequency p and have the meaning of complex amplitudes of the changes in the concentrations. The transition from the time domain to the frequency domain can be done by the Laplace transformation (Milsum, 1966), which in our case results in a simple substitution of "d/dt" by p. For the investigation of frequency responses it is sufficient to use the following identity

$$p=2\pi jf \tag{A3}$$

with f being the frequency, $j=\sqrt{-1}$. The Laplace transform converts Eqs. (A2a)–(A2c) to Eqs. (A4a)–(A4c).

$$pA_3=k_{43}A_4-(k_{34}+k_{32})A_3+k_{23}A_2 \tag{A4a}$$

$$pA_2=k_{32}A_3-(k_{23}+k_{21})A_2+k_{12}A_1 \tag{A4b}$$

$$pA_1=k_{21}A_2-(k_{12}+k_e)A_1. \tag{A4c}$$

Rearranging the above equations leads to the following transfer functions or frequency responses:

$$\frac{A_1}{A_2}=\frac{k_{21}}{(p+k_e+k_{12})} \tag{A5}$$

$$\frac{A_2}{A_3}=\frac{k_{32}(p+k_e+k_{12})}{(p+k_{23}+k_{21})(p+k_e+k_{12})-k_{12}k_{21}} \tag{A6}$$

$$\frac{A_3}{A_4} = \frac{k_{43}\{(p+k_{23}+k_{21})(p+k_e+k_{12})-k_{12}k_{21}\}}{\text{denominator}} \tag{A7}$$

$$\frac{A_2}{A_4} = \frac{k_{43}k_{32}(p+k_e+k_{12})}{\text{denominator}} \tag{A8}$$

$$\frac{A_1}{A_4} = \frac{k_{43}k_{32}k_{21}}{\text{denominator}} \tag{A9}$$

with

$$\text{denominator} = \underbrace{(p+k_{34}+k_{32})}_{\text{new root}} \underbrace{\{(p+k_{23}+k_{21})(p+k_e+k_{12})}_{\text{parabola}} - k_{12}k_{21}\} - \underbrace{k_{23}k_{32}(p+k_e+k_{12})}_{\text{straight line}}. \tag{A10}$$

For the transfer function in Eqs. (A5)–(A9) the following statements are found to hold:

1. All the roots of the denominators (which will be called "poles" or "inverse time constants") are real numbers.

2. In the case of the transfer functions which describe the ratio of subsequent reactants (A_1/A_2, A_2/A_3, and A_3/A_4), the number of the roots of the numerator (called "zeros") is less by one than the number of poles. If zeros are existent (e.g., in A_2/A_3 and A_3/A_4), the zeros and poles are located in such a sequence that they alternate with each other.

3. Transfer functions starting with the same reactant (in this case A_4) have the same poles (due to the same denominator) and differ only by the numerator.

Because it is difficult to calculate the roots of the polynomials of the third degree in the denominator of Eqs. (A7)–(A9), the statements *1* and *2* will be verified by means of the graphs in Fig. A1.

The roots I_1 and I_2 of the denominator of A_2/A_3 are given by the intersections of the parabola $(p+k_{23}+k_{21})(p+k_e+k_{12})$ with the horizontal line $k_{12}k_{21}$. These intersections always exist, and thus statement *1* is verified. I_1 and I_2 are located outside the range between the roots of the parabola being

$$r_1 = -(k_e+k_{12}) \quad \text{and} \quad r_2 = -(k_{23}+k_{21}). \tag{A11a, b}$$

Since r_1 is the zero of A_2/A_3, statement *2* is verified. The roots of the denominator of A_3/A_4 are given by the intersection of the parabola of the third degree having the roots I_1 and I_2 (*see* A_2/A_3) and the new root

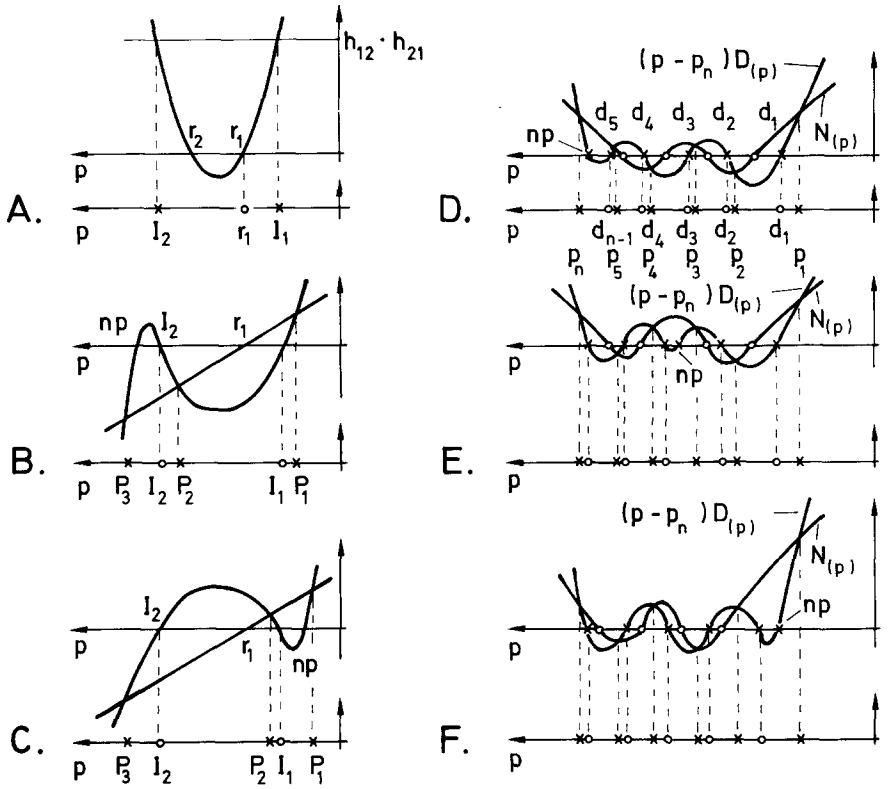

Fig. A1. Generation of the poles (×) and zeros (o) of the transfer function Eq. (A6) (*A*), Eq. (A7) (*B*, *C*), and Eq. (A15) (*D–F*). *B*, *C* and *D–F* differ by the assumption of the location of *np*. In the upper parts of the illustrations the intersections of the parabolas of the denominators are shown, which lead to the configurations displayed on the *p*-axis in the lower parts

$$np = -(k_{34} + k_{32}) \tag{A12}$$

with the straight line crossing the p axis at r_1. r_1 has been shown to be located between I_1 and I_2. The graph in Fig. 1*B* shows that again the new roots p_1, p_2, and p_3 are existent and thus real (statement *1*) and that the zeros of A_2/A_3 (I_1 and I_2) are located between two poles, each (statement 2). In the graph *np* is located at the left hand side of I_2. The situation is not changed significantly, if *np* would be located between r_1 and I_2 (exchange I_2 and *np*).

There is a third and fourth possible location for *np*, i.e., at the right hand side of I_1 or between r_1 and I_1. In these cases which are illustrated in graph *C*, the statements 1 and 2 are verified, too.

Now we have to prove that the statements *1* to *3* hold for a chain of arbitrary length. We shall do so by induction. We assume that the statements *1* to *3* hold for the chains starting with A_n, that means in detail that the transfer function

$$k_{n-1,n} \cdot \frac{A_{n-1}}{A_n} = \frac{N_{(p)}}{D_{(p)}} \tag{A13}$$

fulfills the statement *1* to *3*. Making use of this assumption, we calculate the transfer function A_n/A_{n+1}. The law of mass action leads to the following equation

$$pA_n = k_{n+1,n}A_{n+1} - (k_{n,n+1} + k_{n,n-1})A_n + k_{n-1,n}A_{n-1}. \tag{A14}$$

Inserting Eq. (A13) into Eq. (A14) and rearranging Eq. (A14) leads to

$$\frac{A_n}{A_{n+1}} = \frac{k_{n+1,n}D_{(p)}}{(p + k_{n,n+1} + k_{n,n-1})D_{(p)} - N_{(p)}} = \frac{k_{n+1,n}D_{(p)}}{M_{(p)}}. \tag{A15}$$

The locations of the poles of Eq. (A15) can be determined by means of the graphs in Fig. A1 *D*–*F*. The three graphs differ by the possible locations of the new pole

$$np = -(k_{n,n+1} + k_{n,n-1}) \tag{A16}$$

being at the left hand side of the old poles d_1 to d_{n-1} (graph *D*), in between them (graph *E*) or at the right hand side (graph *F*). In the graph this is shown for 6 poles and 4 zeros; however, it is seen that the sketch holds for an arbitrary number of poles and zeros, because some more swings may be interposed between d_{n-1} and p_5. In any case it can be seen that the statements *1* and *2* are verified.

1. The number of intersections (number of poles) is equal to the degree of the parabola, thus the roots are real numbers (real time constants), and no complex time constants can occur.

2. The poles (p_1 to p_n) and the zeros (d_1 to d_{n-1}) are located in such a sequence that they alternate with each other. A short remark may be worthwhile regarding the intersection p_1 and p_n: The degrees of the parabolas of the numerator and the denominator differ by two, and the sign of the highest coefficient is positive in both cases. Thus the parabola of the denominator has to overtake the parabola of the numerator, creating p_1 and p_n.

3. The proof of the third statement is simple and will not be discussed in detail. It is easily seen that A_n/A_{n+1} and A_{n-1}/A_{n+1} have the

same denominator

$$\frac{A_{n-1}}{A_{n+1}}=\frac{A_{n-1}}{A_n}\cdot\frac{A_n}{A_{n+1}}=\frac{N_{(p)}\cdot k_{n+1,n}D_{(p)}}{D_{(p)}k_{n-1,n}M_{(p)}}=\frac{k_{n+1,n}N_{(p)}}{k_{n-1,n}M_{(p)}}. \tag{A17}$$

The above consideration can be extended to the whole chain showing that all chains starting with A_{n+1} have the same main denominator $M_{(p)}$, and thus all these subchains create only real time constants.

Since the statements *1* to *3* hold for the first three steps and for the step from n to $n+1$, the validity of the three statements is proved for chains of arbitrary length by means of the method of induction. Thus the complex time constants in Table 1 point out the existence of a feedback loop.

A backflow from A_k to A_n with k being less than $n-1$ will be called a feedback loop. If there is a backflow from A_k instead of A_{n-1}, then the number of roots of $N_{(p)}$ is less by 2 or more than the number of roots of $D_{(p)}$. In that case complex roots of the denominator may occur. This is seen from Fig. A1*E*. If, e.g., the root of $N_{(p)}$ adjacent to np is absent (due to the reduced number of roots of $N_{(p)}$) then $(p-pn)D_{(p)}$ may oscillate through the three adjacent roots without crossing $N_{(p)}$. Thus there are two intersections less than expected from the degree of the parabola. In order to complete the number of roots, there has to be a pair of complex roots. Thus it is seen that chains comprising a feedback loop may have complex time constants in contrast to chains without feedback loops.

2. *Proof that Branched Straight Forward Chains, too, Create no Complex Time Constants*

Branching is illustrated by the following arrangement of reactions

$$A_{n+1}\rightleftharpoons A_n\overset{B_m}{\rightleftharpoons}A_{n-1}\rightleftharpoons A_{n-2}\rightleftharpoons\cdots\rightleftharpoons A_1. \tag{A18}$$

$$B_m\rightleftharpoons B_{m-1}\rightleftharpoons\cdots\qquad\qquad\cdots\rightleftharpoons B_1. \tag{A19}$$

The two chains are connected by the reaction

$$A_n+B_m\rightarrow A_{n-1}. \tag{A20}$$

The reactions above lead to the following differential equations

$$\frac{da_n}{dt}=k_{n+1,n}a_{n+1}-k_{n,n+1}a_n+k_{n-1,n}a_{n-1}-k_{n,n-1}b_m a_n \tag{A21}$$

$$\frac{db_m}{dt} = -c_{m,m-1}b_m + c_{m-1,m}b_{m-1} - k_{n,n-1}b_m a_n. \tag{A22}$$

The terms $a_n b_m$ are nonlinear terms. Thus it becomes necessary to make use of the advantages of linearization. All concentrations are split into a steady-state term indexed by an "s" and a variable term indexed by a "v", e.g.

$$a_n = a_n^s + a_n^v \tag{A23}$$

$$a_n b_m = a_n^s b_m^s + b_m^s a_n^v + a_n^s b_m^v + a_n^v b_m^v. \tag{A24}$$

By virtue of the linearization, the terms comprising only steady-state terms can be omitted, because the sum of the steady-state terms has to be zero, and the terms containing more than one factor indexed by "v" can be omitted, because by making the test signal small, the terms of higher order can always be made much less than the linear terms.

Making use of these simplifications Eqs. (A21) and (A22) convert in the frequency domain to (capital letters):

$$pA_n^v = k_{n+1,n}A_{n+1}^v - k_{n,n+1}A_n^v - k_{n,n-1}A_n^s B_m^v - k_{n,n-1}B_m^s A_n^v + k_{n-1,n}A_{n-1}^v \tag{A25}$$

$$pB_m^v = -k_{n,n-1}A_n^s B_m^v - k_{n,n-1}B_m^s A_n^v - c_{m,m-1}B_m^v + c_{m-1,m}B_{m-1}^v. \tag{A26}$$

Due to the proofs displayed above, the transfer functions

$$k_{n,n-1}\frac{A_{n-1}^v}{A_n^v} = \frac{N_{(p)}}{D_{(p)}}, \quad \text{and} \quad c_{m,m-1}\frac{B_{m-1}^v}{B_m^v} = \frac{R_{(p)}}{S_{(p)}} \tag{A27, 28}$$

fulfill statements *1* and *2*.

Thus Eqs. (A25) and (A26) convert to

$$A_n^v\left\{\frac{(p-p_a)D_{(p)} - N_{(p)}}{D_{(p)}} - \frac{c_1 S_{(p)}}{(p-p_b)S_{(p)} - R_{(p)}}\right\} = c_2 A_{n+1}^v. \tag{A29}$$

The meanings of p_a, p_b, c_1, and c_2 can be seen easily from the comparison of Eq. (A29) with Eq. (A25); however, their values are of little interest. Statements *1* and *2* also hold for the following two expressions

$$\frac{D_{(p)}}{M_{(p)}} = \frac{D_{(p)}}{(p-p_a)D_{(p)} - N_{(p)}} \tag{A30}$$

$$\frac{S_{(p)}}{T_{(p)}} = \frac{c_1 S_{(p)}}{(p-p_b)S_{(p)} - R_{(p)}}. \tag{A31}$$

Now, we have to consider the locations of the poles and zeros of Eq. (A32)

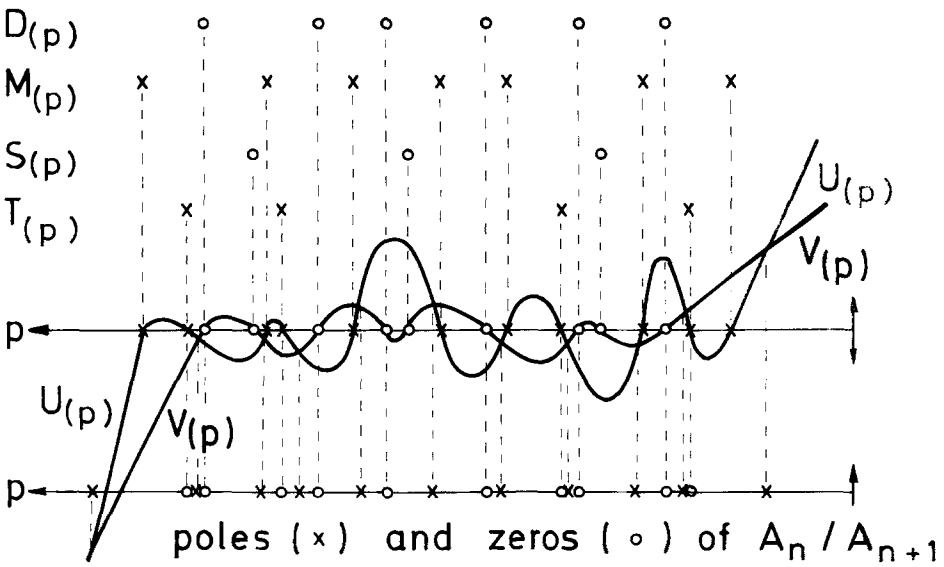

Fig. A2. Generation of the poles (×) and zeros (○) of Eq. (A32)

$$\frac{A^v_{n+1}}{A^v_n} = c_2 \frac{D_{(p)} \cdot T_{(p)}}{M_{(p)} T_{(p)} - D_{(p)} S_{(p)}}. \tag{A32}$$

In Fig. A2 the locations of the roots of $D_{(p)}$, $M_{(p)}$, $T_{(p)}$, and $S_{(p)}$ are drawn. Since statement *2* holds for $D_{(p)}/M_{(p)}$ and $S_{(p)}/T_{(p)}$ never three roots of

$$U_{(p)} = M_{(p)} T_{(p)} \quad \text{(crosses)} \tag{A33}$$

can be adjacent without a root of

$$V_{(p)} = D_{(p)} S_{(p)} \quad \text{(circles)} \tag{A34}$$

in between and vice versa. If there were an interval with three adjacent crosses, two of the crosses would originate from $M_{(p)}$ or $T_{(p)}$. Due to statement *2* applied to Eqs. (A30) and (A31), one circle originating from $D_{(p)}$ or $S_{(p)}$ has to be located between them; thus only one cross originating from $M_{(p)}$ and one from $T_{(p)}$ may be adjacent without a circle between them.

As it is illustrated in Fig. A2, $U_{(p)}$ cannot escape from intersecting with $V_{(p)}$ once per root, because the intersections occur at locations between the roots of $U_{(p)}$ and $V_{(p)}$. There are not more than two roots of one kind unseparated by a root of the other kind, thus each circle has a neighboring cross and thus a neighboring intersection, except for the outside

crosses, but there are intersections because $U_{(p)}$ has to overtake and cross $V_{(p)}$ due to the higher degree. Thus, statement *1* is verified for A_n/A_{n+1}.

In order to verify statement *2* we have to discuss three cases.

1. Two adjacent roots of $D_{(p)}T_{(p)}$ originate from $D_{(p)}$ only. Then there is a zero of $M_{(p)}$ between them due to statement *2* applied to Eq. (A30), and $U_{(p)}$ and $V_{(p)}$ have an intersection between the two roots, which are zeros of Eq. (A32).

2. They originate from $T_{(p)}$. That is similar to the case above.

3. They originate from $T_{(p)}$ and $D_{(p)}$. Then $U_{(p)}$ and $V_{(p)}$ have to intersect between them, too, because $T_{(p)}$ is part of $U_{(p)}$ and $D_{(p)}$ is part of $V_{(p)}$.

Thus it is verified that in the case of branched straightforward reactions statements *1* and *2* are verified.

References

Andrianov, V.K., Bulychev, A.A., Kurella, G.A., Littvin, F.F. 1971. Effect of light on the resting potential and the activity of the cations H^+, K^+, and Na^+ in the vacuolar sap of the cells of *Nitella*. *Biophysics* **16**:1072; *Biofizika* **16**:1031

Berman, M., Weiss, M.F., Shahn, E. 1962. Some formal approaches to the analysis of kinetic data in terms of linear compartmental systems. *Biophys. J.* **2**:289

Bradley, J., Williams, E.J. 1967. Voltage-controllable negative differential resistance in *Nitella* translucens. *Biochim. Biophys. Acta* **135**:1078

Capellos, C., Bielski, B.H.J. 1972. Kinetic Systems. Wiley Interscience, NewYork

Cram, W.J. 1973. Internal factors regulating nitrate and cloride influx in plant cells. *J. Exp. Bot.* **24**:328

Davies, D.D. 1973. Control of and by pH. *Symp. Soc. Exp. Biol.* **27**:513

Davis, R.F. 1974. Photoinduced changes in electrical potentials and H^+ activities of the chloroplast, cytoplasm, and vacuole of *Phaeoceros laevis*. *In:* Membrane Transport in Plants. U. Zimmermann and J. Dainty, editors. pp. 197–201. Springer Verlag, Berlin-Heidelberg-NewYork

Eigen, M. 1968. New looks and outlooks on physical enzymology. *Q. Rev. Biophys.* **1(1)**:3

Eigen, M., Maeyer, L.De. 1963. Relaxation methods. *In:* Techniques of Organic Chemistry. (2nd Ed.) S.L. Friess, E.S. Lewis, A. Weissberger, editors. Vol. 8, Part II, pp. 895–1054. Wiley Interscience, NewYork

Felle, H., Bentrup, F.W. 1976. Effect of light upon membrane potential, conductance, and ion fluxes in *Riccia fluitans*. *J. Membrane Biol.* **27**:153

Flemström, G. 1973. Oscillations of H^+ secretion and electrogenic properties in the isolated frog gastric mucosa. *Biochim. Biophys. Acta* **298**:369

Forsberg, C., 1965. Nutritional studies of *Chara* in axenic cultures. *Physiol. Plant.* **18**:275

Gradmann, D. 1975. Analog circuit of the *Acetabularia* membrane. *J. Membrane Biol.* **25**:183

Gradmann, D., Slayman, C.L. 1975. Oscillations of an electrogenic pump in the plasma membrane of *Neurospora. J. Membrane Biol.* **23**:181

Hansen, U.P. 1967. Zusammenhänge zwischen den Strahlenbeeinflussungen der Membranspannung, der elektrischen Reizschwelle und des ohmschen Widerstandes der Zellmembran von *Nitella flexilis. Atomkernenergie* **12**:447

Hansen, U.P. 1970. Ein digitaler Sinusgenerator für sehr lange Periodendauern. *Elektronik* **19**:221

Hansen, U.P. 1974. Preliminary results of an approach to the quantitative description of the action of light on the membrane potential of *Nitella. In:* Membrane Transport in Plants. U. Zimmermann and J. Dainty editors. pp. 139–145. Springer-Verlag, Berlin-Heidelberg-New York

Hansen, U.P., Keunecke, P. 1974. Comparison of the effects of ionizing irradiation on the electrical parameters in *Nitella* with the effects of visible light. *Atomkernenergie* **23**:5

Hansen, U.P., Keunecke, P. 1977. Parallel pathway in the action of light on membrane potential in *Nitella. In:* Transmembrane Ionic Exchanges in Plants. M. Thellier, A. Monnier, M. Demarty, and J. Dainty, editors. pp. 333–340. C.N.R.S., Rouen/Paris

Hansen, U.P., Slayman, C.L. 1978. Current voltage relationships for a clearly electrogenic cotransport system. *In:* Membrane Transport Processes. Vol. 1, pp. 141–154. J.F. Hoffman, editor. Raven, New York

Hansen, U.P., Warncke, J., Keunecke, P. 1973. Photoelectric effects in *Characean* cells. I. The influence of light intensity. *Biophysik* **9**:197

Heldt, H.W., Werdan, K., Milovancev, M., Geller, G. 1973. Alkalization of the chloroplast stroma caused by light-dependent proton flux into the thylakoid space. *Biochim. Biophys. Acta* **314**:224

Higgins, J. 1967. The theory of oscillating reactions. *Ind. Eng. Chem.* **59**:19

Kishimoto, U. 1966. Hyperpolarizing responses in *Nitella* internodes. *Plant Cell Physiol.* **7**:429

Kitasato, H., 1968. The influence of H^+ on the membrane potential and ion fluxes of *Nitella. J. Gen. Physiol.* **52**:60

Komor, R., Tanner, W. 1977. Transport of hexoses depolarizes the membrane potential of *Chlorella* cells. *In:* Transmembrane Ionic Exchanges in plants. M. Thellier, A. Monnier, M. Demarty, and J. Dainty, editors. pp. 415–421. C.N.R.S., Rouen/Paris

Lee, E.S. 1968. Quasilinearization and estimation of parameters in differential equations. *Ind. Eng. Chem. Fundam.* **7**:152

Lefebvre, J., Gillet, C. 1970. Variations periodiques de la difference de potential electrochimiques des chlorures au cours d'oscillations spontanees du potential de membrane chez *Nitella. Biochim. Biophys. Acta* **203**:575

Lucas, W.J. 1975*a*. Photosynthetic fixation of 14-carbon by internodal cells of *Chara corallina. J. Exp. Bot.* **26**:331

Lucas, W.J. 1975*b*. The influence of light intensity on the activation and operation of the hydroxyl efflux system of *Chara corallina. J. Exp. Bot.* **26**:347

Lucas, W.J. 1976. Plasmalemma transport of HCO_3^- and OH^- in *Chara corallina:* Non-antiporter systems. *J. Exp. Bot.* **27**:19

Lucas, W.J., Dainty, J. 1977. The spatial distribution of OH^- carries along internodal cells of *Chara corallina. In:* Transmembrane Ionic Exchanges in Plants. M. Thellier, A. Monnier, M. Demarty, and J. Dainty, editors. pp. 289–298. C.N.R.S., Rouen/Paris

MacRobbie, E.A.C. 1966. Metabolic effects on ion fluxes in *Nitella translucens.* I. Active influxes. *Aust. J. Biol. Sci.* **19**:363

Metlicka, R., Rybova, R. 1967. Oscillations of the transmembrane potential difference in the alga *Hydrodictyon reticulatum. Biochim. Biophys. Acta* **135**:563

Milsum, J.H. 1966. Biological Control Systems Analysis. McGraw-Hill, New York

Nishizaki, Y. 1968. Rhythmic changes in the resting potential of a single plant cell. *Plant Cell Physiol.* **9**:613

Noyes, H.D., Rehm, W.S. 1971. Unstirred layer model for the long time-constant transient voltage response to current in epithelial tissue. *J. Theor. Biol.* **32**:25

Ogata, K., Kishimoto, U., 1976. Rhythmic change of membrane potential and cyclosis of *Nitella* internode. *Plant Cell Physiol.* **17**:201

Pallaghy, C.K., Lüttge, U. 1970. Light-induced H^+-ion fluxes and bioelectric phenomena in Mesophyll cells of *Atriplex spongiosa*. *Z. Pflanzenphysiol.* **62**:417

Raven, J.A. 1969. Effects of inhibitors on photosynthesis and the active influxes of K and Cl in *Hydrodictyon africanum*. *New Phytol.* **68**:1089

Raven, J.A. 1974. Time course of chloride fluxes in *Hydrodictyon africanum* during alternating light and darkness. *In:* Membrane transport in Plants. U. Zimmermann and J. Dainty, editors. pp. 167–172 and *discussion* p. 246. Springer Verlag, Berlin-Heidelberg-New York

Raven, J.A., and Smith, F.A. 1974. Significance of hydrogen ion transport in plant cells. *Can. J. Bot.* **52**:1035

Raven, J.A., Smith, F.A. 1976. Nitrogen assimilation and transport in vascular land plants in relation to intracellular pH regulation. *New Phytol.* **76**:415

Robinson, J.D. 1968. Regulating ion pumps to control volume. *J. Theor. Biol.* **19**:90

Slayman, C.L., Long, W.S., Lu, C.Y.-H. 1973. The relationship between ATP and an electrogenic pump in the plasma membrane of *Neurospora crassa*. *J. Membrane Biol.* **14**:305

Slayman, C.L., Slayman, C.W. 1968. Net uptake of potasium in *Neurospora*. Exchange for sodium and hydrogen ions. *J. Gen. Physiol.* **52**:424

Slayman, C.L., Slayman, C.W. 1974. Depolarization of the plasma membrane of *Neurospora* during active transport of glucose: Evidence for a proton-dependent cotransport system. *Proc. Nat. Acad. Sci. USA* **71**:1935

Slayman, C.L., Slayman, C.W., Hansen, U.P. 1977. Current-voltage relationships and kinetic models for the glucose/H^+ cotransport system in *Neurospora*. *In:* Transmembrane Ionic Exchanges in Plants. M. Thellier, A. Monnier, M. Demarty, and J. Dainty, editors. pp. 115–122. C.N.R.S., Rouen/Paris

Spanswick, R.M. 1972. Evidence for an electrogenic ion pump in *Nitella translucens*. I. The effect of pH, K^+, Na^+, light and temperature on the membrane potential and resistance. *Biochim. Biophys. Acta* **288**:73

Spanswick, R.M., 1974. Evidence for an electrogenic ion pump in *Nitella translucens*. II. Control of the light-stimulated component of the membrane potential. *Biochim. Biophys. Acta* **332**:387

Strobel, H. 1968. Systemanalyse mit determinierten Testsignalen. VEB Verlag Technik, Berlin

Walker, N.A., Hope, A.B. 1969. Membrane fluxes and electric conductance in *characean* cells. *Aust. J. Biol. Sci.* **22**:1179

Walker, N.A., Smith, F.A. 1975. Intracellular pH in *Chara corallina* measured by DMO distribution. *Plant Sci. Lett.* **4**:125